An Adaptive Resolution Power Flow Algorithm using Graph Signal Processing

Luke Lowery
Dept. of Elec. & Comp. Engineering
Texas A&M University
College Station, TX
lukel@tamu.edu

Adam B. Birchfield
Dept. of Elec. & Comp. Engineering
Texas A&M University
College Station, TX
abirchfield@tamu.edu

***Abstract*—In large power systems, the failed convergence of ac power flow (ACPF) can be challenging to diagnose. This paper presents the Spectral Power Flow (SPF) algorithm, which continuously refines the effective scale of the power flow equations using recent developments in Graph Signal Processing (GSP). The SPF is a sparse, scalable method for adaptively solving ACPF across varying resolutions and is robust to alternative solutions. SPF is designed to solve ACPF over generalized admittance networks, accounting for line shunts and losses. Case studies on 37- and 2000-bus test cases illustrate the speed and efficacy of SPF, marking a new application of GSP for power system studies.**

***Index Terms*—power flow, large power systems, spectral graph wavelet, graph signal processing**

I. Introduction

The convergence of power flow in large power systems is often ill-conditioned. In many stability studies, it can be difficult to obtain a power flow solution near the nominal operating point. Despite the success of sparse methods and nonlinear solvers [1], [2], the non-linearity of power flow can still make convergence difficult in large systems. In larger cases, additional layers of control loops are required to obtain a solution from a flat start.

Perhaps less well studied is the convergence of power flow to *alternate* or *high-energy* solutions, which are mostly not physically realizable. The ability to restore the power flow from alternative solutions is crucial for many stability studies, such as during Geomagnetic Disturbances (GMD), where excessive reactive power loading threatens the voltage stability [3], [4]. Avoiding convergence to an alternative power flow solution in GMD studies remains an active research topic.

Graph-spectral forms of power flow [5], [6] have exclusively been performed in lossless systems, under the decoupled (DC) power flow framework. This is in part because of the necessary conditions of the Spectral Theorem, which cannot be applied to the general $\mathbf{Y}_{\text{bus}}$ matrix due to a lack of an orthonormal decomposition. The authors of these investigations [5], [6] also recognize the infeasibility of calculating the eigenvectors for systems with tens of thousands of buses.

The novel work in [7] shows that, although the voltage magnitude and angle exhibit coherence across the network (large wavelength), the power injection does not. By considering only lossless networks, the authors did not observe that the *losses* exhibit a smooth global structure across the network. Therefore, bus power residuals/losses should be analyzed within the Graph Signal Processing (GSP) framework, rather than bus nodal injections (which are absorbed in a transaction). The spectral approach to angular synchronization over networks is discussed in great detail in [8]. Graph-based resolution iteration [9] has been used theoretically to do multi-resolution analysis for partial differential equations. Lastly, the authors' recent work in [10], [11] employs GSP to identify oscillation modes and to design sparse graph-convolution methods optimized for power systems. These works highlight that the complex bus-admittance matrix $\mathbf{Y}_{\text{bus}}$ is generally unsuitable for standard graph signal processing. Practitioners, therefore, often use a surrogate branch weight to construct the graph Laplacian (e.g., magnitude of the admittance or the squared inverse distance).

In this paper, we derive a novel method to iteratively refine the scale of the power flow solution using tools from the emerging field of GSP [12]. The remainder of the paper is structured as follows. Section II summarizes the necessary background material and notations. Section III analyzes the properties of the power flow in the spectra of the underlying graph. Section IV uses these principles to construct a scale-adaptive power flow algorithm. Section V validates the proposed methods in two case studies.

II. Background

A. Graph Laplacian and Fourier Transform

Let an undirected graph $\mathcal{G} = \{\mathcal{V}, \mathcal{E}, \mathbf{A}, \mathbf{w}\}$ be defined by a set of vertices $|\mathcal{V}| = N$ and a set of edges $\mathcal{E}$ which are related by the arc-node incident matrix $\mathbf{A} \in \mathbb{R}^{|\mathcal{E}|\times|\mathcal{V}|}$ and the vector of branch weights $\mathbf{w} \in \mathbb{R}^{|\mathcal{E}|}$. The *graph Laplacian* (1) is denoted by $\mathscr{L} \in \mathbb{R}^{N\times N}$, a discrete analogue of the continuous Laplace-Beltrami operator.

$$\mathscr{L} := \mathbf{A}^{\top}\text{diag}\left(\mathbf{w}\right)\mathbf{A} \tag{1}$$

A *vertex domain* function on the graph $f : \mathcal{V} \to \mathbb{R}$ can be written as a vector $\mathbf{f} \in \mathbb{R}^{N}$, whose i^{th} element corresponds to the evaluation of f at the i^{th} vertex [13]. For a connected, undirected graph, (1) is positive semi-definite (PSD) with

979-8-3315-8138-1

a real-valued eigenvalue decomposition $\mathbf{U}\mathbf{\Lambda}\mathbf{U}^\top$. The graph Fourier transform (GFT) $\hat{\mathbf{f}}$ of a function $\mathbf{f}$ is given by (2).

$$\hat{\mathbf{f}} := \mathbf{U}^\top \mathbf{f} \tag{2}$$

A function is said to be a *kernel function* $g : \mathbb{R} \to \mathbb{R}$ if it is spectrally defined (3). Let g_a denote the scaled kernel.

$$g_a(\mathscr{L}) = \mathbf{U} g(a\mathbf{\Lambda})\mathbf{U}^\top \tag{3}$$

The convolution of a vertex domain function and a generating kernel (4) corresponds to a product of the two functions in the graph Fourier domain using (3) and (2).

$$\mathbf{f} * g := g(\mathscr{L})\mathbf{f} \tag{4}$$

B. AC and DC Power Flow Notation

We define the state vectors $\mathbf{v}, \theta, \mathbf{p}, \mathbf{q} \in \mathbb{R}^N$ as the voltage magnitude, voltage angle, real power network injection, and reactive power network injection, respectively. The subscript $\mathbf{v}_k$ indicates the k^{th} iteration of the state vector. The Jacobian (5) of the k^{th} iteration is a function of the state vectors at the k^{th} iteration.

$$\mathbf{J}_k := \mathbf{J}(\theta_k, \mathbf{v}_k) = \begin{bmatrix} \partial_\theta \mathbf{p}_k & \partial_V \mathbf{p}_k \\ \partial_\theta \mathbf{q}_k & \partial_V \mathbf{q}_k \end{bmatrix} \tag{5}$$

The DC Power Flow (DCPF) is the lossless linear form of power flow (6) using the branch-susceptance Laplacian $\mathbf{B}$, which takes the form of (1).

$$\mathbf{p} = \mathbf{B}\theta \quad \xrightarrow{GFT} \quad \hat{\mathbf{p}} = \mathbf{\Lambda}\hat{\theta} \tag{6}$$

DCPF can be solved in the graph-spectral domain of $\mathbf{B}$ using the GFT [5], forming a real-valued linearly independent system (6). The following sections will analyze the graph-spectral properties of DCPF and then use GSP to study nonlinear ACPF spectrally.

III. Spectral Properties of the Power Flow

A. The Spectrum of DC Power Flow

The solution to the DCPF can be expressed spectrally (Fig. 1) and is given by (7). Once the angles are obtained for each GFT mode, the vertex domain signal is reconstructed using inverse GFT $\theta = \mathbf{U}\hat{\theta}$.

$$\hat{\theta}(\lambda) = \frac{\hat{p}(\lambda)}{\lambda} \qquad \forall \lambda \neq 0 \tag{7}$$

In DCPF, the power balance must be achieved globally, and there are no transmission losses; the net power injection must be zero ($\mathbf{1}^\top \mathbf{p} = 0$ or $\hat{p}(0) = 0$). Further, the average angle can be arbitrarily chosen to minimize the solution energy (i.e., $\hat{\theta}(0) = 0$) of the steady-state solution (8).

$$\hat{p}(0) = 0 \quad \text{and} \quad \hat{\theta}(0) = 0 \tag{8}$$

Conversely, in lossy ACPF, there may be no nodal reference frame in which the average angle is zero.

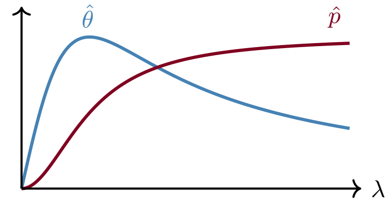

Fig. 1: The spectral DC power flow prior distributions of a steady-state power flow.

B. Shunt Effects on the Voltage Magnitude Spectrum

We generally expect the average voltage to be near the nominal voltage and to be smooth across the underlying graph. In the language of GSP, we can express this as a scaling function subject to the admissibility criteria (9).

$$\hat{v}(0) \approx 1 \qquad \text{and} \qquad \lim_{\lambda \to \infty} \hat{v}(\lambda) = 0 \tag{9}$$

Consider the spectral effects of the transmission line shunt admittance $\mathbf{y}_{\text{sh}}$ on the voltage magnitude. Barring the existence of unlikely distributions of shunts throughout the network, we expect the spectral form of the shunt admittance $\hat{y}_{\text{sh}}$ to take the form of a scaling function as well (Fig. 2).

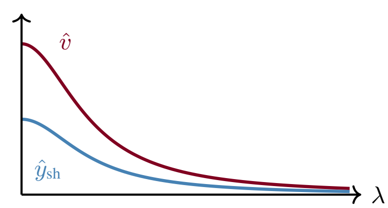

Fig. 2: The prior spectral distributions of voltage and shunt admittance.

For the power flow solution $\mathbf{v}, \theta$ to be unique, it should be phase unambiguous. This is a property of a *minimum phase shift* function (MPS), which is causal, passive, and bijective. The spectral voltage $\hat{v}$ is MPS if there is a one-to-one mapping to the spectral phase $\hat{\theta}$. This indicates that zero crossings or local extrema in the spectral function indicate that the solution is an alternative (spatial harmonic).

C. Regarding Phase-Wrapping and Critical Scale

Using the graph spectral forms of the power flow solution ($\hat{v}$, $\hat{\theta}$), one can interpret alternative power flow solutions as manifestations of phase ambiguity across spatial scales. In particular, when spectral components drive angle updates beyond physically realizable limits, the resulting phase wrapping can yield higher-energy (nonphysical) solutions.

This perspective motivates separating smooth, large-scale voltage-support behavior from the components that primarily affect phase gradients (Fig. 3a–b). Shunt capacitance tends to regularize voltage magnitude by dissipating energy in highly shunted regions, whereas abrupt phase variations manifest as higher-frequency content. From this viewpoint, one can enforce a global structural constraint to discourage excessive

979-8-3315-8138-1

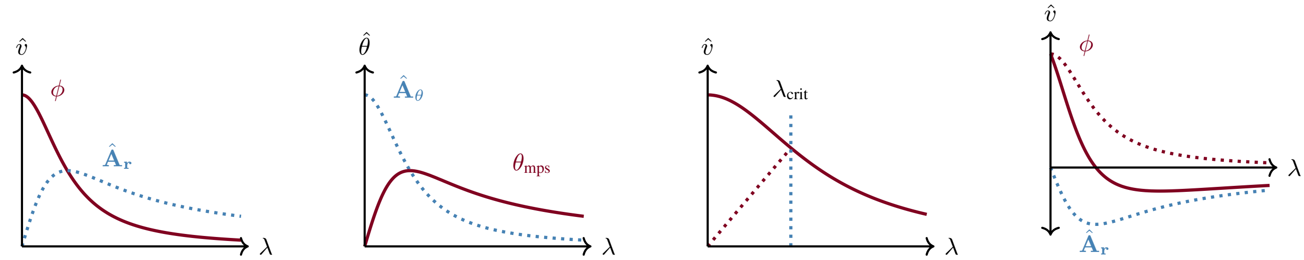

(a) Magnitude Kernel (b) Phase Kernel (c) Critical Scale (d) Phase-Ambiguity

Fig. 3: The spectral kernel functions of (a) the voltage magnitude scalar and vector potentials, (b) the voltage angle stationary and asynchronous component, and (c) the critical scale of the scalar potential, and (d) an example where the vector potential exceeds the critical scale, producing a higher-energy solution.

phase wrapping and reduce the risk of voltage collapse or convergence to alternative solutions (Fig. 3d).

Abstractly, there exists a critical scale at which the phase profile transitions from a wrapped, vortex-like pattern to a smoother, large-scale structure. Therefore, we should enforce dominant (structural) network flows before resolving fine-scale features, so that high-resolution patterns do not form prematurely.

IV. AC Spectral Power Flow

The observations from the previous section are used here to develop a variable-resolution power flow, used to iteratively refine the power flow. The proposed method can easily be integrated into existing power flow solvers, providing a resolution interface between the solver and the network model.

A. Principles of AC Spectral Power Flow

1) Voltage Magnitude: Large-scale reactive power (Q) mismatches shall be prioritized over local-Q mismatches. If one were to attempt to solve local-Q (small-scale) mismatches first, this would risk entering a state in which no phase angle can meet the P demand, leading to an inevitable voltage collapse/explosion in local regions. Thus, we preferentially solve global-Q mismatch first to *restrict* local P-flow patterns from arising (i.e., low voltage, higher-energy solution).

2) Phase Ambiguity: If the linearized power flow step advances the voltage angle more than physically realizable, this manifests as an 'over wrapped' potential (Fig. 3d), violating causality. The spectral scale of the over-wrapping (Fig. 3c) is called the *critical scale*, where structural collapse of the function can occur within the network. To discourage this, P mismatches are sequentially resolved from smallest to largest scales, prioritizing local P flows before losses arise. This is not unlike the process of simulated annealing.

3) Spectral Power Transactions: The scaling function component of the complex power injections represents the transmission losses (Fig. 4c). Unlike the lossless case, the energy dissipated into the network is detectable using scaling functions (i.e., unbalanced injection). Conversely, transactions of power over the network must be detectable using high-pass filters, which correspond to balanced vertex-domain injections. Using graph filters, the 'lossy' and 'transactional' mismatches across the network can be measured at any chosen scale.

B. Extrema of Spectral Functions

We identify the scale at which the nodal power mismatch is maximized to determine the optimal scale/resolution for updating the state vector. To do so, we define the functional ζ which returns the set of eigenvalues where $\hat{f}$ is maximized.

$$\zeta(f) := \underset{\lambda}{\operatorname{argmax}}\, \hat{f}(\lambda) \tag{10}$$

This is surprisingly aligned with the spirit of Levenberg-Marquardt methods [1], [2] which scale the Jacobian by the norm of the mismatch vector $||\mathbf{f}||$. This functionally acts as a low-pass filter on the Jacobian, selecting the linear sensitivities that are likely to be global in scale.

$$\max_{\lambda} \hat{f}(\lambda) \approx \max_{s} ||\mathbf{f} * \Psi_s|| \tag{11}$$

Extrema of a graph-spectral function can be approximated (11) using the Spectral Graph Wavelet Transformation (SGWT), the graph equivalent of filter banks. Using the sparse techniques, the peak scale can be identified in milliseconds for an 80k-bus case [10].

C. Adaptive Scale Power Flow Algorithm

The following algorithm is designed using GSP and observations from the previous sections to improve ACPF's convergence. Although any feasible initial state could be used, a flat start initial guess $\mathbf{v}_0 = \mathbf{1}\angle 0$ is used in the case study, corresponding to the largest possible scale.

Step One: Approximate the step in voltage coordinates to the power flow solution using Newton-Raphson (NR), where $\Delta\mathbf{p}_k, \Delta\mathbf{q}_k$ are the real and reactive bus mismatch of the k^{th} iteration, respectively. This can be obtained using an existing power flow solver.

$$\begin{bmatrix}\Delta\mathbf{p}_k\\ \Delta\mathbf{q}_k\end{bmatrix} = \mathbf{J}_k \begin{bmatrix}\mathrm{d}\theta_k\\ \mathrm{d}\mathbf{v}_k\end{bmatrix} \tag{12}$$

Step Two: Determine the resolution at which the power flow needs to be refined using (13). $A \in \mathbb{R}$ is the smallest scale of P mismatch, corresponding to the spectral P maxima

979-8-3315-8138-1

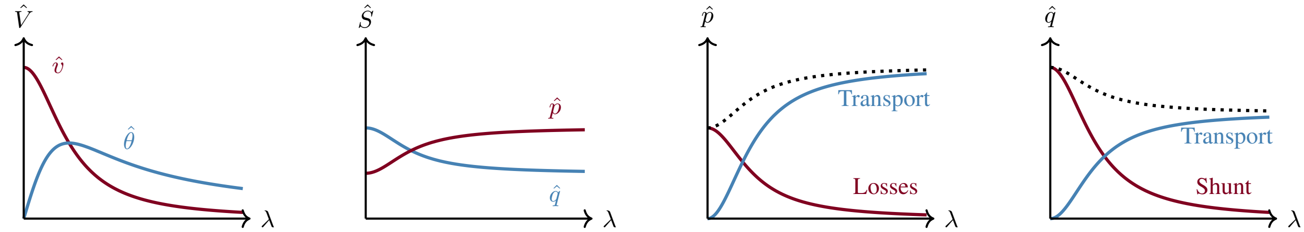

(a) Phasor Priors (b) Total Complex Power (c) Real Power (d) Reactive Power

Fig. 4: The AC power flow spectral density functions of (a) the complex voltage signal, (b) the complex power over the network, (c) the real power in the network, (d) the reactive power in the network.

with the largest eigenvalue. $B \in \mathbb{R}$ is the largest scale of Q mismatch, corresponding to the spectral Q maxima with the smallest eigenvalue. This preferentially selects local-P and global-Q, masking global-P and local-Q features.

$$\frac{1}{A} = \max \zeta(\Delta \mathbf{p}_k) \qquad\qquad \frac{1}{B} = \min \zeta(\Delta \mathbf{q}_k) \tag{13}$$

Step Three: Update the state vector using the filtered sensitivities (14) at the solving scale A and B for voltage magnitude and angle, respectively. Let μ_A and ϕ_B be high- and low-pass graph filters scaled by A and B, respectively.

$$\begin{aligned} \theta_{k+1} - \theta_k &= \mathrm{d}\theta_k * \mu_A \\ \mathbf{v}_{k+1} - \mathbf{v}_k &= \mathrm{d}\mathbf{v}_k * \phi_B \end{aligned} \tag{14}$$

The scaled iteration step (14) is applied to all buses except the slack bus, whose magnitude and angle remain constant. Additionally, only the angle θ is updated for PV-type buses, which have a constant voltage magnitude.

V. Case Study

We apply the adaptive Spectral Power Flow (SPF) on the synthetic Hawaii 37-bus and Texas 2000-bus cases [14] to demonstrate its properties and advantages. The implementation of low-, high-, and band-pass graph filters is discussed in [11] in detail (e.g., low-pass filter $\phi(\lambda) = 1/(1+\lambda)$). Lastly, the admittance-magnitude Laplacian is used for each case.

A. Synthetic Hawaii

Before the adaptive-scale method is applied to the synthetic Hawaii case, we apply a smooth-scale transition of the proposed algorithm as follows: At each iteration, the scale of the voltage magnitude low-pass filter ϕ_A is decreased, gradually transitioning from the largest ($A >> 1$) to the smallest ($A << 1$) scale. Likewise, the scale of the voltage-angle high-pass filter, μ_B, is gradually increased, transitioning from the smallest ($B << 1$) to the largest ($B >> 1$). This iterative process (Fig. 5) shows how the solution evolves as the resolution increases.

Then, the adaptive SPF of Section IV-C is performed using the scale update rule (13). The iterative solution (Fig. 6) takes a similar path to the smoothed descent (Fig. 5). The algorithm improves convergence by 'jumping' to critical power flow scales where the mismatch is most significant.

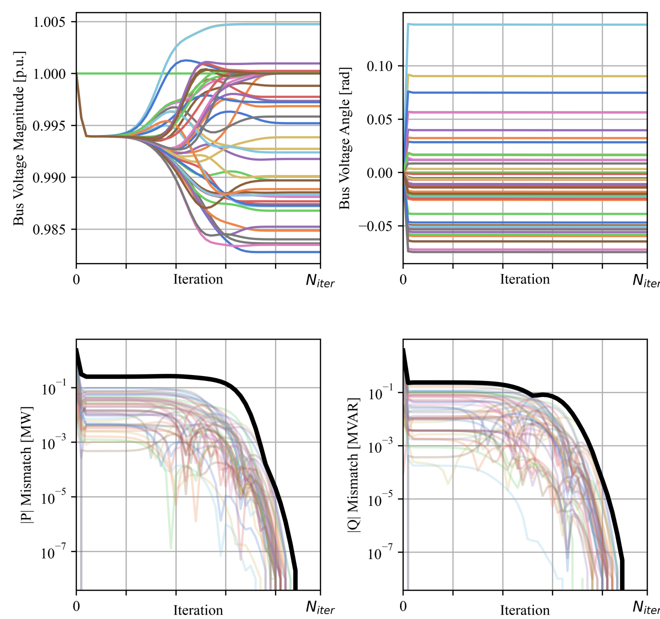

Fig. 5: The iterative values of the bus voltage magnitude (top left) and angle (top right) of the Hawaii case using a smooth scale progression. The bus mismatch of real (bottom left) and reactive (bottom right) power demonstrates convergence.

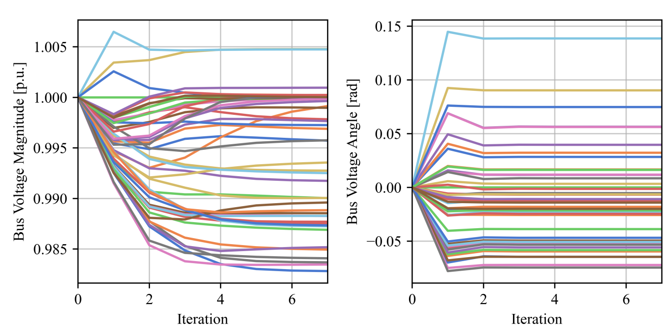

Fig. 6: Adaptive SPF per iteration on the Hawaii case, showing the voltage magnitude (left) and angle (right).

979-8-3315-8138-1

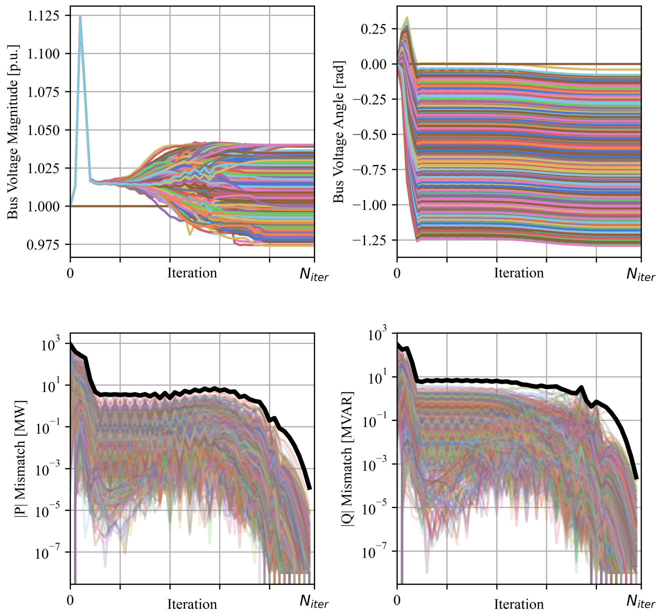

Fig. 7: The iterative values of the bus voltage magnitude (top left) and angle (top right) of the Texas case using a smooth scale progression. The bus mismatch of real (bottom left) and reactive (bottom right) power demonstrates convergence.

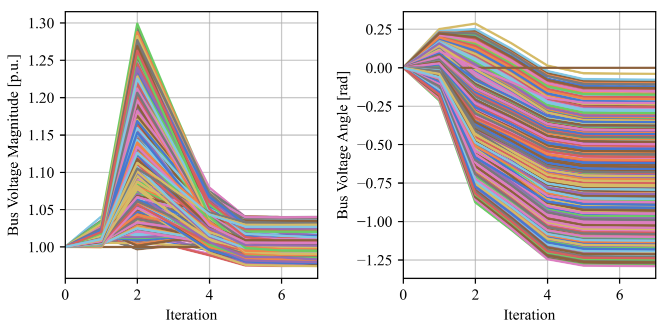

Fig. 8: Adaptive SPF per iteration on the Texas case, showing the voltage magnitude (left) and angle (right).

B. *Synthetic Texas*

The algorithm is applied to the Texas case to demonstrate its scalability to larger networks. As done in the Hawaii case, the iterative scale-smoothing procedure is performed first (Fig. 7). We see the voltage angle approach its final solution much earlier in the refinement than the voltage magnitude.

Using the full adaptive SPF, the power flow solution enters a region of attraction after four iterations (Fig. 8). Notably, this procedure is compatible with the control loops of tools such as PowerWorld. This algorithm can be implemented within the innermost solution loop, so it does not interfere with control loop features such as LTC or PV-type bus switching.

VI. Conclusion

The novel Spectral Power Flow (SPF) algorithm refines the resolution of the ac power flow (ACPF) by leveraging concepts from Graph Signal Processing (GSP). An adaptive variation of SPF is designed to optimally adjust the resolution of bus mismatches while solving the power flow. The sparse implementation of SPF is practical for large cases exceeding tens of thousands of buses. The case study demonstrates that the SPF procedure can achieve ACPF convergence in large, poorly conditioned systems by enforcing solution smoothness on the underlying graph.

The proposed methods do not rely upon lossless network assumptions and are physically meaningful. In future work, the ability of the proposed methods to prevent divergence will be quantified extensively across varying case sizes, loading conditions, and graph filter types.

In an era of increasingly complex power systems, stability studies may find some respite in the advancements of GSP. Despite the shared challenges of power systems and GSP, applications of the emerging field are largely unexplored. The successful application of spectral graph filters to improve power flow convergence in large power systems highlights the promising marriage of these fields.

References

[1] R. Pourbagher and S. Y. Derakhshandeh, "A powerful method for solving the power flow problem in the ill-conditioned systems," *International Journal of Electrical Power & Energy Systems*, vol. 94, pp. 88–96, 2018.

[2] P.-J. Lagacé, M.-H. Vuong, and I. Kamwa, "Improving power flow convergence by newton raphson with a levenberg-marquardt method," in *2008 IEEE Power and Energy Society General Meeting-Conversion and Delivery of Electrical Energy in the 21st Century*, IEEE, 2008.

[3] L. Lowery and A. B. Birchfield, "Voltage stability in plausible non-uniform geomagnetic disturbances," *IEEE Trans. Power Syst.*, 2025.

[4] K. S. Shetye, T. J. Overbye, A. B. Birchfield, J. D. Weber, and T. L. Rolstad, "Computationally efficient identification of power flow alternative solutions with application to geomagnetic disturbance analysis," in *2020 IEEE Texas Power and Energy Conference (TPEC)*, IEEE, 2020.

[5] N. Retiére, D. T. Ha, and J.-G. Caputo, "Spectral graph analysis of the geometry of power flows in transmission networks," *IEEE Systems Journal*, vol. 14, no. 2, pp. 2736–2747, 2019.

[6] F. Koeth, *Investigations of spectral properties in power systems*. PhD thesis, Université Grenoble Alpes, 2019.

[7] L. Dabush, A. Kroizer, and T. Routtenberg, "State Estimation in Partially Observable Power Systems via Graph Signal Processing Tools," *Sensors*, vol. 23, p. 1387, Jan. 2023.

[8] M. Fanuel and R. Bardenet, "Sparsification of the regularized magnetic laplacian with multi-type spanning forests," *Applied and Computational Harmonic Analysis*, p. 101766, 2025.

[9] L. Migus, Y. Yin, J. A. Mazari, and P. Gallinari, "Multi-scale physical representations for approximating pde solutions with graph neural operators," 2022.

[10] L. Lowery, J. Baek, and A. Birchfield, "Using spectral graph wavelets to analyze large power system oscillation modes," *59th Hawaii International Conference on System Sciences (HICSS)*, 2026. Preprint available at https://birchfield.engr.tamu.edu/publications.

[11] L. Lowery and A. B. Birchfield, "Spectral graph filters for large power systems," in *2026 IEEE Texas Power and Energy Conference (TPEC)*, Feb. 2026. Preprint available at https://birchfield.engr.tamu.edu/publications/.

[12] L. Stanković and E. Sejdić, *Vertex-frequency analysis of graph signals*. Springer, 2019.

[13] D. I. Shuman, S. K. Narang, P. Frossard, A. Ortega, and P. Vandergheynst, "The emerging field of signal processing on graphs: Extending high-dimensional data analysis to networks and other irregular domains," *IEEE Signal Process. Mag.*, vol. 30, May 2013.

[14] A. B. Birchfield, T. Xu, K. M. Gegner, K. S. Shetye, and T. J. Overbye, "Grid structural characteristics as validation criteria for synthetic networks," *IEEE Transactions on Power Systems*, vol. 32, no. 4, 2017.

979-8-3315-8138-1